NeuroImage 179 (2018) 403–413

Contents lists available at ScienceDirect

NeuroImage

journal homepage: www.elsevier.com/locate/neuroimage

Establishing the functional connectivity of the frontotemporal network in pre-attentive change detection with Transcranial Magnetic Stimulation and event-related optical signal

Chun-Yu Tse [a,b,*], Long-Yin Yip [a,b], Troby Ka-Yan Lui [a,b], Xue-Zhen Xiao [a,b], Yang Wang [a,b], Winnie Chiu Wing Chu [c], Nathan Allen Parks [d], Sandra Sau-Man Chan [e], Sebastiaan Franciscus Wijnandus Neggers [f]

[a] Department of Psychology, The Chinese University of Hong Kong, Hong Kong SAR, China
[b] Center for Cognition and Brain Studies, The Chinese University of Hong Kong, Hong Kong SAR, China
[c] Department of Imaging & Interventional Radiology, The Chinese University of Hong Kong, Hong Kong SAR, China
[d] Department of Psychological Science, University of Arkansas, Fayetteville, AR, USA
[e] Department of Psychiatry, The Chinese University of Hong Kong, Hong Kong SAR, China
[f] Brain Center Rudolf Magnus, Department of Psychiatry, University Medical Center Utrecht, The Netherlands

ARTICLE INFO

Keywords:
TMS
EROS
Functional connectivity
MMN
Change detection
Frontotemporal network

ABSTRACT

Current theories of pre-attentive deviant detection postulate that before the Superior Temporal Cortex (STC) detects a change, the Inferior Frontal Cortex (IFC) engages in stimulus analysis, which is particularly critical for ambiguous deviations (e.g., deviant preceded by a short train of standards). These theories rest on the assumption that IFC and STC are functionally connected, which has only been supported by correlational brain imaging studies. We examined this functional connectivity assumption by applying Transcranial Magnetic Stimulation (TMS) to disrupt IFC function, while measuring the later STC mismatch response with the event-related optical signal (EROS). EROS can localize brain activity in both spatial and temporal dimensions via measurement of optical property changes associated with neuronal activity, and is inert to the electromagnetic interference produced by TMS. Specifically, the STC mismatch response at 120–180 ms elicited by a deviant preceded by a short standard train when IFC TMS was applied at 80 ms was compared with the STC mismatch responses in temporal control (TMS with 200 ms delay), spatial control (sham TMS at vertex), auditory control (TMS pulse noise only), and cognitive control (deviant preceded by a long standard train) conditions. The STC mismatch response to deviants preceded by the short train was abolished by TMS of the IFC at 80 ms, while the STC responses remained intact in all other control conditions. These results confirm the involvement of the IFC in the STC mismatch response and support a functional connection between IFC and STC.

Introduction

The sound of a fire alarm is automatically detected and captures attention even when one is fully engaged in reading a newspaper with music playing in the background. This phenomenon illustrates the brain's constant monitoring for environmental threats and is commonly known as pre-attentive or automatic change detection. These unexpected changes elicit an event-related brain potential (ERP) component called the mismatch negativity (MMN; Näätänen et al., 2007; Näätänen and Michie, 1979). In laboratory settings, the MMN is usually studied using passive auditory oddball paradigms. In these paradigms, rare deviant stimuli embedded randomly in a train of frequent standard stimuli are presented to the participants while their attention is directed elsewhere (e.g., on a silent subtitled movie, a book, or a cognitive task).

MMN associated responses in both left and right superior temporal cortices (STC) and right inferior frontal cortex (IFC) have been consistently observed with functional magnetic resonance imaging (fMRI; Doeller et al., 2003; Molholm et al., 2005; Opitz et al., 2002; Rinne et al., 2005), electrocorticography (ECoG; Dürschmid et al., 2016; Phillips et al., 2016), magnetoencephalography (MEG; Rinne et al., 2000),

* Corresponding author. Department of Psychology & Center for Cognition and Brain Studies, The Chinese University of Hong Kong, 328 Sino Building, CUHK, Shatin, N.T., Hong Kong SAR, China.
E-mail address: cytse@psy.cuhk.edu.hk (C.-Y. Tse).

https://doi.org/10.1016/j.neuroimage.2018.06.053
Received 20 March 2018; Received in revised form 5 June 2018; Accepted 17 June 2018
Available online 19 June 2018

electroencephalography with source localization analysis (EEG; Deouell et al., 1998; Giard et al., 1990; Rinne et al., 2000; Shalgi and Deouell, 2007), and optical brain imaging methods (Rinne et al., 1999; Tse and Penney, 2007, 2008; Tse et al., 2006, 2013, 2015). Although there is a consensus in the field that the STC mismatch response reflects a process comparing the current and expected events (Näätänen et al., 2007; Winkler, 2007), a number of competing hypotheses about the possible role of the IFC have been suggested (e.g., contrast enhancement, Opitz et al., 2002; predictive model, Winkler, 2007).

According to the contrast enhancement hypothesis (Opitz et al., 2002), the IFC processes incoming auditory stimuli such that when the difference between the current and the expected event is small or ambiguous, it amplifies the difference. Hence, an increase in IFC activity is expected before the comparison process occurs in the STC (Tse and Penney, 2008; Tse et al., 2013). Under the predictive coding framework (Friston, 2005, 2010, 2011) and the predictive model hypothesis (Winkler, 2007), regularities from the auditory environment are extracted to construct a model for predicting the incoming events. The IFC is involved in the extraction or reactivation of the prediction model for the later STC comparison process. Although these hypotheses suggest different functional roles for the IFC, both assume that the IFC engages in stimulus analysis before the comparison or detection stage in the STC. In other words, a functional connection between the IFC and the STC is a basic assumption of both hypotheses. However, due to the correlational nature of brain imaging, the functional connectivity between IFC and STC cannot be established based on a co-activation pattern of the two brain regions. To address this issue, we examined the functional connectivity between IFC and STC in the change detection process by disturbing the right IFC with single pulse Transcranial Magnetic Stimulation (spTMS) during stimulus presentation and simultaneously measuring the left STC response with an optical brain imaging method, the event-related optical signal (EROS; Gratton, 2010; Gratton et al., 1995; Gratton and Fabiani, 2001, 2009).

EROS measures the change in optical properties associated with shifts in membrane potential during neuron depolarization and hyperpolarization (Foust and Rector, 2007; Rector et al., 1997, 2005) and has temporal and spatial resolution in the millisecond and sub-centimeter range, respectively. Hence, EROS is fundamentally different from functional near-infrared spectroscopy (fNIRS), which measures the hemodynamic response, similar to the fMRI BOLD signal. The EROS mismatch responses in the IFC and STC, which is conceptualized as the optical counterpart of the ERP MMN, have been consistently elicited by various types of deviance, including time of occurrence and omission (Sable et al., 2007; Tse and Penney, 2007; Tse et al., 2006), frequency (Tse and Penney, 2008), duration (Rinne et al., 1999; Tse et al., 2013), and audiovisual speech sound (Tse et al., 2015). EROS mismatch responses in the IFC and STC correlate with simultaneously recorded ERP MMN responses (Tse and Penney, 2008; Tse et al., 2013). The IFC response to ambiguous deviants began approximately 80 ms after stimulus onset and the STC response began after approximately 120–180 ms (Tse and Penney, 2008; Tse et al., 2013). This activation sequence is consistent with the contrast enhancement and predictive model hypotheses that IFC is involved in the initial stage of change detection. However, observing the predicted activation sequence of IFC and STC is not sufficient to support a causal relationship or functional connection between the two brain regions. For example, the observed activation sequence could be produced by a third brain region driving the effects in both IFC and STC, but with different time delays. TMS modulates cortical activity by inducing a focal current in the cortex at a specific time and location through electromagnetic induction and thereby permits examination of the putative functional connectivity between the frontal and temporal cortices. Specifically, IFC function can be disrupted to determine whether and how the later mismatch response at STC is modulated.

A number of brain imaging methods, including EEG/ERP (Bonato et al., 2006; Ilmoniemi et al., 1997) and fMRI (Baudewig et al., 2001; Bestmann et al., 2004; Bohning et al., 1999; de Weijer et al., 2014; Van Ettinger-Veenstra et al., 2009), have been used to monitor the modulation of brain activity by TMS. A similar approach was adopted to study the ERP MMN, however, these previous TMS MMN studies (Möttönen et al., 2013; Oshima et al., 2017) focused on the involvement of motor and parietal cortices in change detection rather than the frontotemporal network underlying MMN generation. Other MMN studies used transcranial direct-current stimulation (tDCS) to investigate the frontal and temporal generators of MMN (Chen et al., 2014; Impey and Knott, 2015; Weigl et al., 2016). tDCS applies a direct electric current on the scalp to modulate neuron excitability. MMN amplitude was reduced with the anodal tDCS electrode on the frontal cortex (Chen et al., 2014; Weigl et al., 2016), but enhanced with the anodal tDCS electrode on the temporal cortex (Impey and Knott, 2015). To avoid electromagnetic interference induced by tDCS and TMS, brain stimulation and EEG recording were typically carried out in separate blocks in these studies (Chen et al., 2014; Impey and Knott, 2015; Oshima et al., 2017; Weigl et al., 2016). However, establishing the functional connectivity with timing specificity between the frontal and temporal cortices requires the STC mismatch response to be recorded immediately after the IFC stimulation.

Therefore, the ideal brain imaging method for monitoring the brain response triggered by TMS or tDCS should be inert to the electromagnetic interference produced by the stimulator and excellent in localizing brain activity spatially and temporally: EROS fulfils both of these requirements (Parks, 2013). The possibility of simultaneous TMS and fNIRS (Hada et al., 2006; Kozel et al., 2009; Mochizuki et al., 2006), as well as TMS and EROS recording (Parks, 2013; Parks et al., 2015, 2012) have been demonstrated empirically. However, no study to date has combined TMS with EROS to investigate the functional relationship between the IFC and STC, especially in pre-attentive change detection.

Here, spTMS was applied on the IFC 80 ms after the deviant onset (i.e., 80 ms from deviant onset to the onset of TMS pulse), while the EROS mismatch response was recorded from STC at 120–180 ms. If the IFC and STC are functionally connected and the IFC is critical for the later comparison process in STC, then disrupting the IFC should abolish the STC mismatch response. However, in the absence of a functional connection between the frontal and temporal cortices, disrupting the IFC would not affect the STC mismatch response.

By comparing the brain responses when TMS is applied to different brain regions or time windows, spatial and temporal specificity can be established. However, these comparisons alone cannot establish functional connectivity between two brain regions, because the difference in responses could be due to the different stimulation protocols and not the specific TMS effect on cognitive function. A cognitive control condition with a TMS protocol identical to the experimental condition is required (de Graaf and Sack, 2011) to establish the functional connection between IFC and STC. Here, the cognitive control condition was achieved by varying the number of preceding standards in order to affect the degree of IFC engagement.

Both the contrast enhancement and prediction model hypotheses predict that the IFC plays a more critical role in the processing of deviants preceded by a short rather than a long standard train. Previous studies (Baldeweg et al., 2004; Bendixen et al., 2007; Bendixen and Schröger, 2008; Haenschel et al., 2005; Vossel et al., 2011; Winkler et al., 1996) demonstrated that standard train length modulates MMN amplitude. Frontal cortex activity was found to increase when detecting unpredictable change (Dürschmid et al., 2016), and decrease with increasing standard train length (Vossel et al., 2011). A short train of standards provides limited information to establish a stable and precise model for predicting future events compared to a long standard train. Therefore, the IFC is needed to enhance the difference between the incoming deviant and the poorly established predictive model; or more effort is needed to activate the less-well defined predictive model in IFC. However, a deviant preceded by a long standard train requires less enhancement or effort from the IFC in the pre-comparison stage.

In this study, the STC mismatch responses elicited by deviants with different numbers of preceding standards were compared when TMS was

applied on the IFC, on the vertex for sham stimulation, or when only the TMS pulse noise was presented. The STC mismatch responses were also compared when TMS or TMS pulse noise was presented at the pre-comparison stage of 80 ms or the post-comparison stage of 200 ms to establish the temporal specificity of the TMS effect. We predicted that TMS applied on IFC with an 80 ms delay from the deviant onset should abolish the later STC mismatch response for a deviant following a short standard train, while the STC mismatch response for deviants following a long standard train should remain intact. The STC mismatch responses should also be observed in other conditions (i.e., when TMS was applied on IFC with 200 ms delay from deviant onset, when sham TMS was applied on vertex with 80 or 200 ms delay, or when TMS pulse noise was presented with 80 or 200 ms delay).

Methods

Participants

Twenty-four university students (13 females; age 18–23 years, mean age 21.1 years) participated after giving informed consent. The study was approved by The Joint Chinese University of Hong Kong - New Territories East Cluster Clinical Research Ethics Committee. All participants were screened for TMS contraindication (Rossi et al., 2009; Wassermann, 1998), right-handed according to the Edinburgh Handedness Inventory (Oldfield, 1971), reported having normal hearing, normal or corrected-to-normal vision, and no history of neurological disorders. The participants watched a self-selected silent movie with subtitles, and were told to ignore auditory events during the experiment.

Stimuli and experimental design

There were four block types: IFC TMS, Vertex TMS Control, Auditory Control, and Equal Probability Control (Fig. 1). The IFC TMS, Vertex TMS Control, and Auditory Control blocks shared the same auditory passive oddball design. The standard and deviant stimuli were 392 Hz pure tones (musical notes G4; 80% of trials) and 440 Hz pure tones (musical notes A4; 20% of trials), respectively. The frequency difference between the deviant and standard is considered small or ambiguous based on previous parametric MMN studies (Alho et al., 1994; Liebenthal et al., 2003; Tse and Penney, 2008). The tone duration was 50 ms including 5 ms rise and fall periods. Tone stimulus onset asynchrony (SOA) was 1500 ms and tones were presented in pseudorandom order with the constraint that deviants were preceded by 2–8 standards. For analysis, the deviants following 4 to 7 standards were assigned to either the short (4 or 5) or long (6 or 7) standard train conditions (8.33% of total trials for each group).

The majority of the deviants were preceded by 4–7 standards, while the remaining deviants (3.34% of total trials) were preceded by 2, 3, or 8 standards to produce variability in the train length. Due to the limited number of trials (i.e., 10 trials for 2–3 standards, and 6 trials for the 8 standards), the deviants preceded by 2, 3, or 8 standards were not included in the analysis. The range of the standard train length was limited by the total deviant probability. As multiple control conditions were included for establishing the functional, spatial, and temporal specificity of the TMS effect, while the duration of the experiment had to be kept within a reasonable range, a relatively high deviant probability of 20% was used.

Each block type was repeated 3 times to present a total of 960 trials for each condition (768 standards and 192 deviants) or a total of 3840 trials for the entire experiment. Auditory stimuli were presented using the MATLAB software (MathWorks, Inc., Natick, USA) and the Psychophysics Toolbox (Brainard, 1997) through a pair of ER2 in-ear type earphones (Etymotic Research, Elk Grove Village, IL, USA) at a comfortable intensity, (i.e., about 70 dB).

Half of the standard and deviant tones were randomly paired with the application of a TMS pulse at 80 ms after the tone onset, while the other half were paired with a TMS pulse at 200 ms after tone onset. Half of the trials (40 trials) at each TMS pulse delay (80 vs. 200 ms) comprised a short standard train and the other half a long standard train. The 80 ms delay was selected because this corresponds to the time window of the early IFC optical MMN effect, whereas the 200 ms delay was selected because it is after the STC optical MMN response (i.e., post-comparison stage; Tse and Penney, 2008; Tse et al., 2006, 2013). The 200 ms delay condition served as a within-block control to confirm whether any TMS effect obtained in the 80 ms delay condition is specific to the pre-comparison stage.

Depending on the block type, TMS coils with different locations and orientations producing real TMS, sham TMS, and TMS pulse noise were paired with the standard and deviant tones. The TMS pulses paired with the standards were designed to produce TMS pulse noise, but no direct TMS effect on the brain; while the TMS pulses paired with the deviants were designed to produce real TMS effect on IFC, sham TMS, or TMS pulse noise. However, the TMS pulses for the 80 and 200 ms delay conditions were identical for the same type of stimuli (standard or deviant) within a particular block type.

In the IFC TMS block, the deviants were paired with TMS pulses applied at right IFC from the deviant TMS coil, while the standards were paired with TMS pulses applied from a second TMS coil located vertically

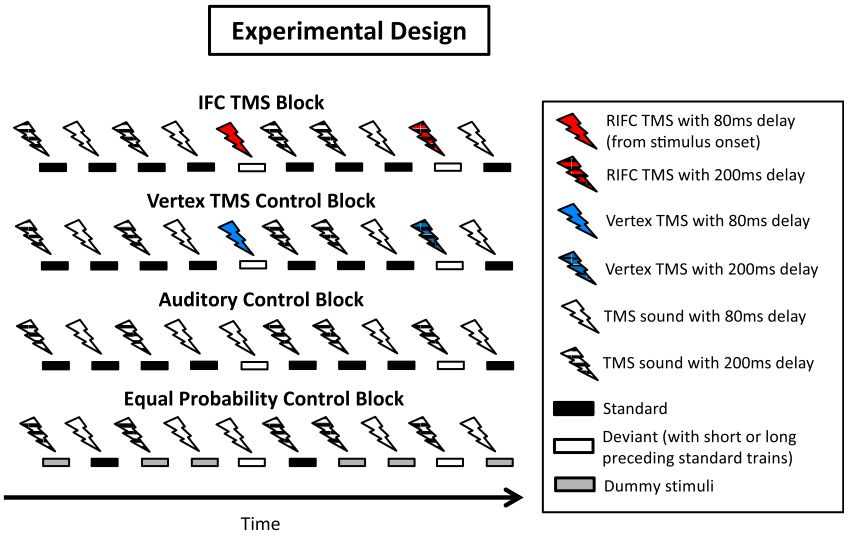

Fig. 1. Illustration of the stimuli properties and TMS procedure in the IFC TMS, Vertex TMS Control, Auditory Control, and Equal Probability Control Blocks.

above the deviant coil and with the same orientation as the deviant coil (Fig. 2A). The standard TMS coil was used to minimize differences in the background auditory environment during presentation of the standard and deviant stimuli (i.e., to ensure that any MMN elicited is not attributable to TMS pulse noise, but due to the change in pitch or frequency of the deviant).

Simultaneous TMS and EROS over the same brain area is possible using a special head-mount for the optical fibers to reduce or eliminate mechanical interference between the TMS coil and EROS recording (Parks, 2013; Parks et al., 2012). However, limited space for positioning the optical fibers and TMS coil and vibration of the TMS coil interfering with the optical signal recording is potentially problematic. Previous studies indicated predominant right IFC and bilateral STC activities in pre-attentive change detection (Leff et al., 2009; Szycik et al., 2013; Tse and Penney, 2007; Tse et al., 2012), particularly for frequency deviants (Liebenthal et al., 2003; Opitz et al., 2002), so we avoided these measurement difficulties by applying TMS to the right frontal cortex while EROS mismatch response was recorded from the left STC only. Structural connections between IFC and STC (Frühholz and Grandjean, 2013; Frühholz et al., 2015) and between bilateral temporal cortices (Hofer and Frahm, 2006) have been revealed using Diffusion Tensor Imaging (DTI), which supports the feasibility of stimulating and imaging the brain activities in opposite hemispheres.

The Vertex TMS Control block was similar to the IFC TMS block except for the location of the deviant TMS coil, which was positioned on the vertex to control for non-location specific TMS effects. In other words, if the optical MMN effect at STC in the IFC TMS block is abolished, while the optical MMN effect at STC is preserved in the Vertex TMS Control block, the absence of an STC response in the experimental block can be attributed to the specific TMS effect at IFC.

The Auditory Control block was designed to demonstrate the typical optical MMN response in the absence of TMS, but in an auditory environment similar to the IFC TMS and Vertex TMS Control blocks. The positions and orientations of the TMS coils were basically identical to the IFC TMS block, however, the orientation of the deviant coil differed from the IFC TMS block by rotating it so that the magnetic field pointed away from the brain.

The design of the Equal Probability Control block and the locations of the two TMS coils were similar to that of the Auditory Control block. However, three other tones (493 Hz, B4; 523 Hz, C5; and 587 Hz, D5) in addition to the tones serving as the standard and deviant in the other blocks were presented in the Equal Probability Control block. The five types of tone were presented randomly with equal probability (i.e., 20%) which was identical to the deviant probability in the other blocks. By subtracting the EROS response of the physically identical tone (with an identical number of preceding tones and TMS pulse/sound delay) presented in the Equal Probability Control block from the deviants presented in other blocks, the EROS mismatch response without a sensory adaption confound could be recorded (Jacobsen and Schröger, 2001). Blocks belonging to the same block type were presented in succession to shorten the time required for repositioning the TMS coils. The presentation order of the block types was counterbalanced across participants.

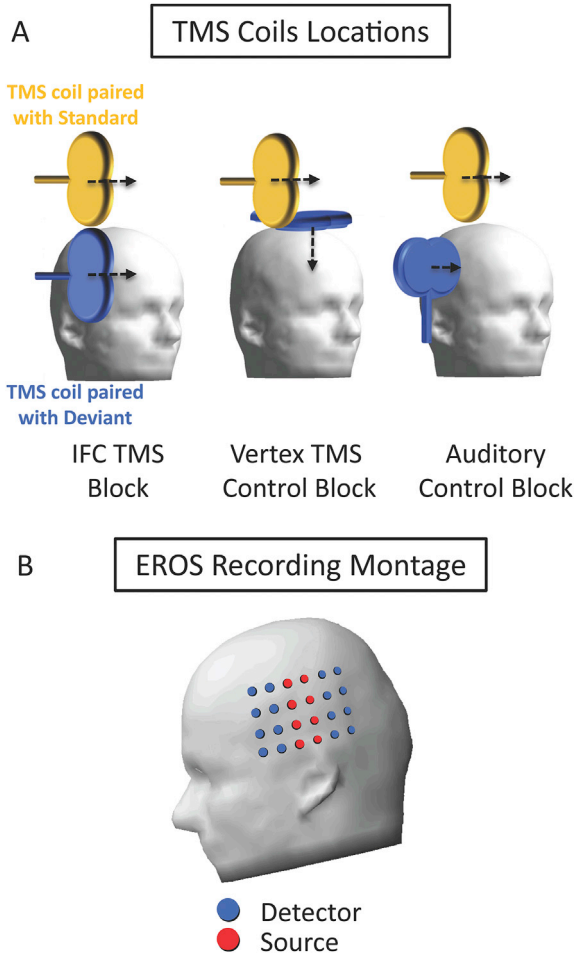

Fig. 2. (A) The placement of TMS coils for the IFC TMS, Vertex TMS Control, and Auditory Control blocks. The yellow and blue color coils indicate the locations and orientations of coils paired with the standard and deviant stimuli, respectively. (B) Montage for EROS recording. The blue and red circles indicate the locations of detector and source optical fibers.

Transcranial magnetic stimulation

TMS was administered with two mono-phasic single pulse TMS stimulators (Neuro-MS/D, Neurosoft, Ivanovo, Russia) and two angulated 100 mm figure-of-eight coils. One of the stimulators controlled the TMS coil paired with the deviants, while the other stimulator controlled the TMS coil paired with the standards. Stimulation intensity was set at 80% of each participant's motor threshold, which has been shown to produce a functional disruption or temporary lesion on the targeted brain region leading to the abolishment of the subsequent behavioral or brain responses (Corthout et al., 2000; Davey et al., 1994).

To identify the motor threshold for each participant, the location of the hand region in the right motor cortex was determined by using the 5-cm rule. The TMS coil was first set at the location 5 cm to the right of vertex, with the coil oriented 45° pointing toward the midline and tangential to the scalp surface. The location of the hand region was fine-tuned by shifting the TMS coil along an imaginary grid in steps of approximately 1 cm. The search for motor threshold started with TMS intensity set at 30% of the stimulator's total output and increased in steps of 5% of the total output. Resting motor threshold was identified by the minimum stimulator intensity producing visible movement in the wrist, hand, or any finger in 40–60% of trials for at least 8 consecutive trials.

During the experiment, a neural navigator system (Brain Science Tools BV, Utrecht, The Netherlands; www.neuralnavigator.com) was used to position the TMS coil over the right IFC and the EROS recording montage over the left STC (Fig. 2B) based on the structural MRI of that individual participant. The structural MRI of each individual participant in native space was first transformed to Talairach space to obtain the native space-to-Talairach space transformation matrix. This transformation matrix was inverted and used to reverse transform the Talairach coordinates of the target locations based on previous EROS studies (Tse and Penney, 2008; Tse et al., 2013, 2015) to the native space for each participant by using the software AFNI (Cox, 1996). The coordinates of the target locations in the native space were then entered into the neural navigator system to position the TMS coil and EROS recording montage. The stimulation intensity and the exact stimulation location were adjusted to reduce discomfort due to jaw or facial muscle movement, if necessary. However, the minimum stimulation intensity

was kept higher than 75% of the motor threshold and the stimulation location was kept within 10 mm of the targeted IFC coordinates (Talairach coordinates: x = 60, y = 29, z = 14; Tse and Penney, 2008; Tse et al., 2013, 2015).

EROS recording and analysis

The EROS recording procedure was similar to that used in previous EROS MMN studies (see Fig. 1 in Tse et al., 2010). A frequency domain oximeter (Imagent, ISS, Inc., Champaign, IL, USA) recorded the fast optical signals. Intensity modulated (110 MHz) near infrared light (830 nm) was produced by laser diodes and carried to participants' scalp through plastic-clad silica optical fibers (2.5 m long; 400 μm diameter core). Light emitted from the source fibers passed through the participant's scalp, skull, and brain, and was collected by fiber optic detector bundles (3 mm diameter) back to the oximeter's photomultiplier tubes (PMTs). This signal from the detector bundles was mixed with a 110.003125 MHz signal, generating a signal with a cross-correlational frequency of 3125 Hz, which was sampled at 50 kHz by the analog-to-digital converter. The output signal was fast Fourier transformed (FFT) to compute the DC intensity, AC intensity, and relative phase delay measures. As a previous study (Gratton et al., 2006) reported better sensitivity in measuring EROS with the phase delay measure, only phase delay data were analyzed in this study.

Source and detector optical fibers were secured at the left STC region with a custom-built head-mount. Previous studies consistently demonstrated bilateral temporal cortex activity in the auditory pre-attentive change detection process (Leff et al., 2009; Scherg et al., 1989; Szycik et al., 2013; Tse and Penney, 2007). Due to limited space for the placement of the TMS coil and head mount for optical recordings on the right side of the head, and to improve the EROS sampling rate for combined TMS-EROS application, EROS was recorded from the left STC only. The optical recording montage (Fig. 2B) consisted of 16 detectors and 8 sources producing 128 source-detector pairs. Each light source was turned on for 1.6 ms meaning it took 12.8 ms to cycle through the 8 light sources and to sample the entire area covered by the recording montage (i.e., sampling at 78.125 Hz).

The functional optical data was co-registered with the structural MRI of each participant (Tse et al., 2010; Whalen et al., 2008). These T-1 weighted structural MRIs with the nasion and pre-auricular points marked by Beekley Spots (Beekley Corporation, Bristol, CT) were obtained using a high-field 3.0 T whole-body scanner (Achieva TX, Philips Healthcare, Best, the Netherlands) with an eight-channel head coil. The three-dimensional locations of the fiducial points, the source and detector fibers, as well as 150 points scattered around the scalp and ocular regions, were recorded using a 3D digitizer (Polhemus Fastrak 3Space, Colchester, VT) during the EROS session and co-registered with the MR anatomical data using a surface fitting method (Whalen et al., 2008). The locations of the source and detector fibers were used for the reconstruction of the expected light path for each channel and participant in a common Talairach space (Talairach and Tournoux, 1988).

The optical data were corrected for phase wrapping, normalized, pulse corrected (Gratton and Corballis, 1995), and filtered with a 0.01–10 Hz band-pass filter, then averaged for each time point, channel, condition, and participant separately using a 100 ms pre-stimulus baseline. Channels with a source-detector distance shorter than 20 mm were excluded from the analysis, as the shallow light path only passes through the scalp, but not the brain (Gratton et al., 2006). Noisy channels with a source-detector distance longer than 50 mm or phase variability (i.e., standard deviation of a channel across trials and time points) over 160 picoseconds were excluded from analysis. The averaged data for each channel were reconstructed into the voxel space data and statistical parametric map for analysis using the Opt-3D software (Gratton, 2000). Specifically, the optical signal for a given voxel was calculated from the mean value of the channels that overlapped at that particular voxel for each participant (Wolf et al., 2000) and *t* statistics were computed across participants for each voxel and converted to *z*-scores. As the EROS signal was recorded from the left hemisphere, only data from the middle sagittal plane to the surface of the left hemisphere could be included in the analysis. The statistical parametric map (SPM) in Talairach space was projected onto the left lateral view of a template brain with the application of an 8 mm (FWHM) spatial filter for each time point of 12.8 ms. Region of Interest (ROI) and Interval of Interest (IOI) statistical analyses of the EROS data were based on previous EROS MMN studies (Tse and Penney, 2007, 2008; Tse et al., 2006, 2013) with corrections for multiple comparisons using the random field theory approach (Friston et al., 1994). Talairach coordinates of brain response on the y (anterior–posterior) and z (inferior–superior) axes were reported for statistical maps with a lateral projection view.

Statistical parametric mapping (SPM) analyses were conducted on the EROS mismatch responses for deviants following the short and long standard trains in the IFC TMS, Vertex TMS Control, and Auditory Control blocks from 127 to 217 ms. Two interaction effect contrasts examining the difference in EROS mismatch responses elicited by the short and long standard train deviants between the Vertex TMS and Auditory Control blocks (i.e., [(Short Train Deviant - Long Train Deviant) $_{\text{in Vertex TMS Control Block}}$ - (Short Train Deviant - Long Train Deviant) $_{\text{in Auditory Control Block}}$]) and between IFC TMS and the average of Vertex TMS and Auditory Control blocks (i.e., [(Short Train Deviant - Long Train Deviant) $_{\text{in IFC TMS Block}}$ - (Short Train Deviant - Long Train Deviant) $_{\text{average of Vertex TMS and Auditory Control Block}}$]) were also included in the SPM analyses. SPM analyses were conducted separately for conditions with TMS pulse delays of 80 and 200 ms.

Repeated measures ANOVA with the factors Train Length (short and long), Block Type (IFC TMS, Vertex TMS Control, and Auditory Control), and TMS Pulse Delay (80 and 200 ms) were conducted on the peak EROS responses within the ROI and IOI of each condition. Follow-up repeated measures ANOVAs and t-tests (2-tailed) were conducted to compare differences in EROS mismatch responses between the short and long train length conditions for each block type and TMS pulse delay. Greenhouse-Geisser correction was applied with the epsilon (ε) correction factor when appropriate.

Results

EROS STC mismatch responses from 127 to 217 ms after the deviant onset projected on the left lateral view of a template brain are shown in Fig. 3. Consistent with the predicted results, no statistically significant STC mismatch response was observed for the short train deviant when TMS was applied on IFC with 80 ms delay. However, significant STC mismatch responses were found in all other conditions (i.e., long train deviants with IFC TMS at 80 ms, short and long train deviants with IFC TMS at 200 ms, short and long train deviants with vertex TMS at 80 and 200 ms, and short and long train deviants with TMS pulse noise presented at 80 and 200 ms in the auditory control block). The interaction contrast comparing the difference in STC mismatch responses of the IFC TMS block and the averaged Vertex TMS and Auditory Control blocks was statistically significant for 80 ms TMS pulse delay, but not for 200 ms TMS pulse delay. The interaction contrast comparing the difference in STC mismatch responses of the Vertex TMS and Auditory Control Blocks was not significant for TMS pulse delays of 80 or 200 ms. The *Z* scores, critical *Z* value, and locations of the peak EROS STC mismatch responses are summarized in Table 1.

Repeated measures ANOVA with the factors Train Length (short and long), Block Type (IFC TMS, Vertex TMS Control, and Auditory Control), and TMS Pulse Delay (80 and 200 ms) on the peak EROS mismatch responses of each condition showed significant main effects of Train Length (F (1,23) = 5.02, p = .035, *partial eta square,* (η_p^2) = .18), and Block Type (F (2,46) = 4.32, p = .019, η_p^2 = .16), while the main effect of TMS Pulse Delay (F (1,23) = 0.29, p = .595, η_p^2 = .01) was not statistically significant. The Train Length x TMS Pulse Delay interaction (F (1,23) = 4.50, p = .045, η_p^2 = .16) was significant, while neither the Train Length x Block

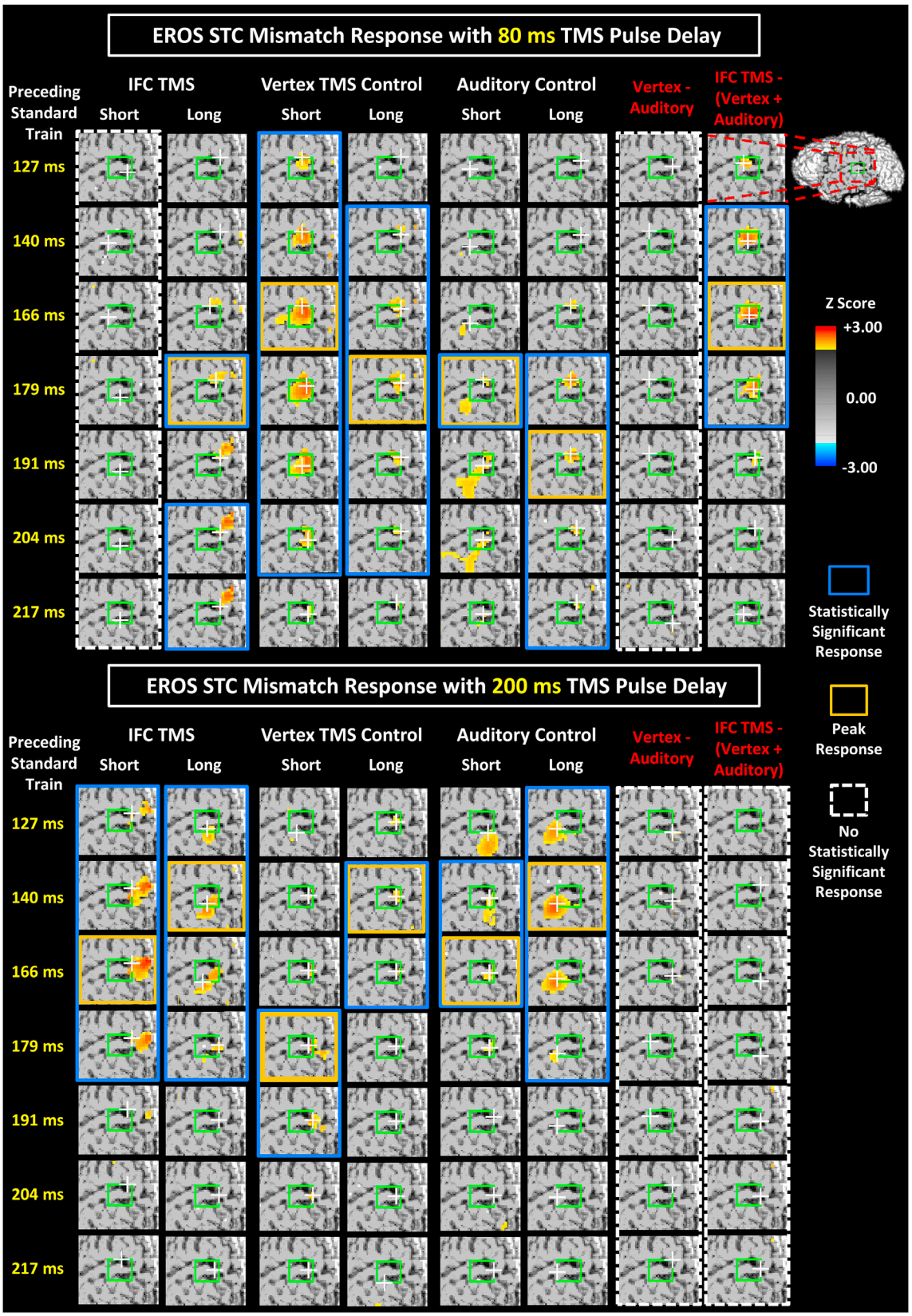

Fig. 3. Statistical maps of the EROS STC mismatch responses overlaid on the left lateral views of a template brain. The columns present the EROS responses from 127 to 217 ms, with a time window of 12.8 ms, after stimulus onset for the deviants with short or long standard trains in the IFC TMS, Vertex TMS Control, and Auditory Control blocks. The last two columns present the responses for the interaction contrasts comparing the differences in mismatch response of deviants with short and long standard trains between the Vertex TMS and Auditory Control block, and between IFC TMS block and the average of the two control blocks. The upper and lower panels show the results for TMS with 80 and 200 ms delay. Darker grey color on the template brain shows the recording areas covered by the optical montage. The green box indicates the region of interest. White cross indicates the location of the peak mismatch response.

Table 1
Peak EROS STC mismatch responses.

Block Type	IFC TMS		Vertex TMS Control		Auditory Control		Vertex TMS -Auditory Control	IFC TMS - (Vertex TMS + Auditory Control)
Preceding Standard Train	Short	Long	Short	Long	Short	Long	Short - Long	Short - Long
TMS Pulse Delay							80 ms	
Peak *Z* (Critical *Z*)	1.86 (2.33)	2.17* (2.12)	2.79* (2.15)	2.88* (2.28)	2.23* (2.19)	2.58* (2.44)	0.99 (2.27)	2.76* (2.48)
Peak Latency (ms)	191	166	153	166	166	179	153	153
Talairach Coordinate (y, z)	−41, 2	−48, 17	−43,17	−51, 14	−43, 17	−43, 17	−31, 17	−43, 9
TMS Pulse Delay							200 ms	
Peak *Z* (Critical *Z*)	2.86* (2.29)	2.58* (2.22)	2.57* (2.45)	2.49* (2.38)	2.36* (2.14)	2.65* (2.23)	1.81 (2.55)	1.43 (2.49)
Peak Latency (ms)	153	140	166	140	153	140	140	179
Talairach Coordinate (y, z)	−51, 14	−41, 2	−48, 9	−48, 9	−48, 7	−31, 2	−51, 4	−51, 7

Note: * indicates Peak Z > Critical Z with $p < .05$ with correction for multiple comparisons.

Type interaction, (F (2,46) = 0.96, $p = .392$, $\eta_p^2 = .04$), nor the Block Type x TMS Pulse Delay interaction, (F (2,46) = 2.15, $p = .128$, $\eta_p^2 = .09$), were statistically significant. Most importantly, the Train Length x Block Type x TMS Pulse Delay interaction was statistically significant (F (2,46) = 5.67, $p = .006$, $\eta_p^2 = .20$).

Follow-up repeated measures ANOVAs with the factors Train Length and Block Type were carried out separately for TMS pulse delays of 80 and 200 ms (Fig. 4). For the 80 ms TMS pulse delay, the main effects of Train Length (F (1,23) = 9.57, $p = .005$, $\eta_p^2 = .29$) and Block Type (F (2,46) = 3.82, $p = .029$, $\eta_p^2 = .14$), as well as their interaction (F (2,46) = 5.53, $p = .012$, $\varepsilon = .80$, $\eta_p^2 = .19$), were statistically significant. A follow-up *t*-test showed a smaller STC mismatch response elicited by short train deviants compared to long train deviants in the IFC TMS block (t (23) = −3.99, $p < .001$, *Cohen's d* (d) = .81). However, no significant difference in STC mismatch responses was found for short and long train deviants in the Vertex TMS Control (t (23) = −0.73, $p = .473$, $d = .15$) and Auditory Control blocks (t (23) = −1.04, $p = .309$, $d = .21$). The difference in STC mismatch responses between short and long train deviants was larger in the IFC TMS block than in the Vertex TMS Control (t (23) = −2.46, $p = .022$, $d = .50$) and Auditory Control blocks (t (23) = −3.02, $p = .006$, $d = .62$), but not between the Vertex TMS Control and Auditory Control block (t (23) = 0.34, $p = .736$, $d = .07$).

For the 200 ms TMS pulse delay, the main effects of Train Length (F (1,23) = 0.13, $p = .725$, $\eta_p^2 = .005$) and Block Type (F (2,46) = 1.91, $p = .160$, $\eta_p^2 = .08$), as well as the Train Length x Block Type interaction (F (2,46) = 1.67, $p = .206$, $\varepsilon = .78$, $\eta_p^2 = .07$), were not statistically significant. No difference in STC mismatch response was found between short and long train deviants in the IFC TMS (t (23) = 1.62, $p = .119$, $d = .33$), Vertex TMS Control, (t (23) = −0.81, $p = .426$, $d = .17$), or Auditory Control (t (23) = .77, $p = .449$, $d = .16$) blocks. Similar results were shown by follow-up repeated measures ANOVAs with the factors Train Length and TMS Pulse Delay carried out separately for the three block types. A statistically significant Train Length x TMS Pulse Delay interaction was found in the IFC TMS block only (F (1,23) = 16.92, $p < .000$, $\eta_p^2 = .42$), but not in the Vertex TMS Control (F (1,23) = .11, $p = .741$, $\eta_p^2 = .01$) or Auditory Control blocks (F (1,23) = 1.13, $p = .299$, $\eta_p^2 = .05$).

These results demonstrate that IFC processes occurring at the pre-comparison stage (i.e., at 80 ms) play a critical role in eliciting the later STC mismatch response when the deviant follows a short standard train compared to a long standard train. The spatial and temporal specificity of the TMS effects were established by comparing mismatch responses between IFC TMS and sham Vertex TMS, and between the TMS pulses with 80 and 200 ms delay, respectively. Comparison between the IFC TMS and Auditory Control blocks further suggested that the IFC TMS effect on STC mismatch response could not be produced merely by the difference in TMS pulse noise between standard and deviant stimuli.

No statistically significant STC EROS mismatch response was found earlier than 127 ms when the TMS pulses was applied at 80 or 200 ms in all conditions. As shown in Fig. 3 (lower panel), STC EROS mismatch response was absent at 204–230 ms when TMS pulse was applied at 200 ms. These results suggested the absence of immediate TMS effect on STC at the moment when TMS pulses were applied or mechanical artifact produced by the TMS application.

Discussion

The current study examined the functional connectivity between IFC and STC in change detection by using a passive oddball paradigm in conjunction with spTMS disruption of IFC function at the pre-comparison stage and recording the later STC mismatch response with EROS. The STC mismatch response of deviants preceded by a short standard train was abolished by TMS on IFC at 80 ms after the deviant onset, while STC mismatch response of deviants preceded by a long standard train remained intact. In addition, STC mismatch responses were also consistently observed when TMS was applied to the IFC at 200 ms, or when sham TMS at vertex or TMS pulse noise was delivered at 80 and 200 ms, and no difference in the STC mismatch responses between short and long train deviants was found in these conditions. These results demonstrate a critical functional role of IFC in eliciting the later STC mismatch response in the pre-attentive or automatic change detection process when the deviants are preceded by a short train of standards.

Functional connectivity between the frontal and temporal cortices is a common assumption behind hypotheses explaining the IFC mismatch response in passive oddball paradigms. Under the predictive account of change detection (Garrido et al., 2008, 2009), a predictive model is built by minimizing the discrepancy between the predicted and actual events (i.e., the prediction error) across a series of trials. The IFC and STC are suggested to be hierarchically organized with feedforward and feedback functional connections for building the model (Gratton, 2018). The prediction error is reflected by mismatch responses in the IFC and STC elicited by deviant events. Previous support for the feedforward and feedback functional connections between the IFC and STC were mainly based on correlational modeling of ECoG, MEG, and EROS data (Phillips et al., 2016; Tse et al., 2013). The current study provides empirical evidence supporting the functional connection between the frontal and temporal cortices by direct manipulation of brain function. The functional connection between IFC and STC is also assumed under the contrast enhancement hypothesis, in which IFC is involved in enhancing the difference between ambiguous deviants and standards during the change detection process. This hypothesis does not contradict the predictive model account of change detection because the standards can also be interpreted as the regularity encoded in the model.

A short standard train provides limited samples to illustrate the invariant properties, or the regularity pattern, of the standard. The predictive model built on such limited information is also less reliable. Consistent with both hypotheses, at the pre-comparison stage the IFC could be involved in the enhancement process to differentiate the deviant from the highly variable regularity pattern or unstable predictive model.

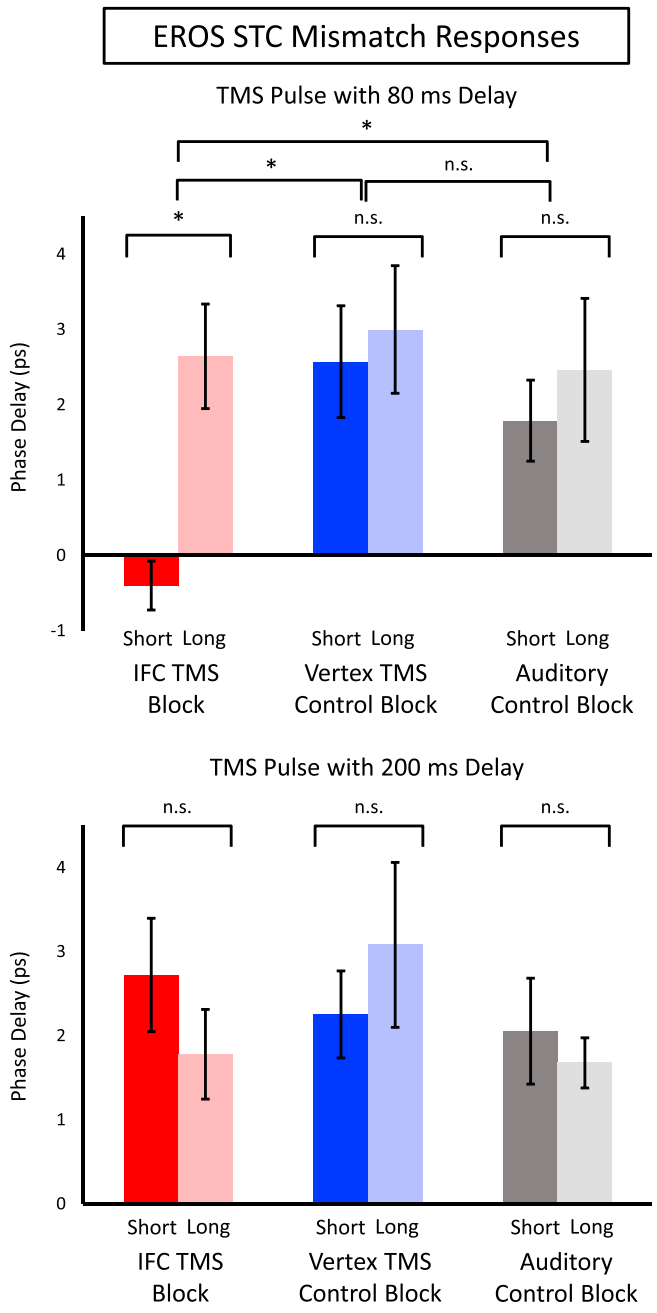

Fig. 4. Peak amplitude of the averaged EROS mismatch response within the region and interval of interest for the deviants with short or long standard trains elicited in the IFC TMS, Vertex TMS Control, and Auditory Control blocks. The upper and lower panels show the results for TMS with 80 and 200 ms delay. Error bars indicate the SEM computed across participants. * indicates $p < .05$; *n.s.* indicates non-significant difference.

Therefore, disrupting IFC function at the pre-comparison stage with TMS may upset the contrast enhancement process and result in failure to elicit a subsequent STC mismatch response.

Studies using other brain imaging methods found a IFC and STC mismatch response pattern consistent with the current study. A ECoG study (Dürschmid et al., 2016) showed both frontal and temporal cortex mismatch responses in detecting unpredictable change with a random number of standard tones preceding the deviant tone, while only a temporal cortex mismatch response was found in detecting predictable change with a fixed number of standard tones preceding the deviant tone. A fMRI study (Vossel et al., 2011) found a decrease in right IFC activity level to standard stimuli with increasing standard train length. The current study extended these findings by showing the functional connectivity between IFC and STC by directly manipulating the IFC activity level.

Differential modulation of IFC and STC responses by deviance properties in the change detection process was demonstrated in the current study, implying that the IFC and STC mismatch responses should not be conceptualized as a single unit in MMN generation. Previous EROS studies (Tse and Penney, 2008; Tse et al., 2013) found an early IFC mismatch response, before the STC mismatch response, for ambiguous deviants; while only a STC mismatch response, without an early IFC mismatch response, was elicited by salient deviants. A previous EEG source localization study also suggested unequal contribution of the frontal and temporal sources to the generation of the MMN. The frontal source contributed more variance to the MMN generation than the temporal source in a complex paradigm as compared to their relative contributions in a simple oddball paradigm (MacLean et al., 2015). MEG studies on music pattern violations found a frontal mismatch response to violations of the more complex melodic pattern, but not to violations of the relatively simple rhythmic pattern (Lappe et al., 2013a, 2013b). The IFC mismatch response was consistently observed with less well-established regularities and/or ambiguous deviants. These findings may help to explain the mixed results in identifying the IFC generator of MMN (Deouell, 2007) and the non-linear change in MMN amplitude with deviance level (Horváth et al., 2008; Tiitinen et al., 1994).

The single-pulse TMS protocol adopted in this study produced a functional disruption or temporary lesion on the targeted brain region leading to the abolishment of subsequent behavioral or brain responses (Plewnia et al., 2003). Conclusions based on the absence of a behavioral or brain response triggered by TMS are potentially problematic. A null behavioral or brain response could be produced by a number of factors, including incorrect stimulation location, weak stimulation intensity, and insufficient statistical power, rather than the real TMS effect (de Graaf and Sack, 2011). The current study addressed this issue by following the design and analyses procedure recommended by de Graaf and Sack (2011).

First, the latencies and locations to stimulate IFC and to record the STC mismatch response were determined based on previous EROS studies (Tse and Penney, 2007, 2008; Tse et al., 2006, 2012, 2013, 2015). A neural navigation system was used for the placement of the TMS coils and the EROS recording montage based on the structural MRI of the individual participant for improved spatial accuracy (Neggers et al., 2004). The coil positions were monitored and maintained within a 1 cm radius of the targeted locations during the experiment to maximize the TMS effect on IFC and to capture the STC mismatch response.

Second, the interpretation of the results does not depend on the absence of a STC mismatch response in a single condition (i.e., IFC TMS at 80 ms in the processing of short train deviants). Our conclusion is based on the differences in STC mismatch responses between different stimulation protocols in the experimental and control blocks. Sham TMS at vertex served as a control location to demonstrate the spatial specificity of TMS effect on IFC. A no TMS control condition (i.e., auditory control block) was included to show that the observed TMS effect could not be produced by the TMS pulse noise alone. The 200 ms delay TMS pulse condition was introduced to examine the temporal specificity of the TMS effect and determine whether the TMS effect is produced by a general change in brain excitability during the entire experimental block. Most importantly, the TMS effect is demonstrated by the difference in STC mismatch responses between short and long train deviants under identical TMS protocols. Long train deviants served as a cognitive control condition to demonstrate the disruption of a specific cognitive process in change detection by TMS. In fact, STC mismatch responses were reliably recorded across multiple conditions, the null response in a single condition is unlikely to be due to insufficient statistical power, but rather the disruption of IFC function by TMS.

Only TMS pulse noise, but no real TMS, was paired with the stimuli in the Equal Probability Control block to control for the confound that TMS

pulse noise may elicit MMN in the experimental and other control blocks. Due to the difference in the orientation of the TMS coils, TMS pulse noise in the Equal Probability Control block may still be different from the IFC TMS and Vertex TMS Control blocks producing different auditory and somatosensory experiences associated with the TMS. However, it is unlikely that the difference in the auditory and somatosensory experiences could produce the observed result pattern. Due to the 80 ms delay of TMS pulses after deviant onset, the sensory and mismatch responses produced by the difference in auditory and somatosensory experiences are expected at around 180–280 ms, which is 100–200 ms after TMS application. As the EROS STC mismatch response typically started before 144 ms and peaked from 144 to 166 ms, it is unlikely to be contaminated by the brain responses associated with different auditory and somatosensory experiences. In addition, our conclusion is further protected from this unlikely confound by comparing the STC mismatch responses of deviants with different standard train length, but under identical stimulation protocol.

Previous studies (Baldeweg et al., 2004; Bendixen et al., 2007; Bendixen and Schröger, 2008; Haenschel et al., 2005; Vossel et al., 2011; Winkler et al., 1996) demonstrated larger MMN amplitudes for deviants preceded by longer standard trains (i.e., more than 10 versus 5 standards). However, in our study, no difference in the EROS STC mismatch responses was found between deviants with short and long standard trains in the Vertex TMS and Auditory Control blocks. In order to accommodate all of the control conditions while keeping the total duration of the experiment within a reasonable range, the standard train length was limited to 2 to 8 standards, with most of the trains in the 4 to 7 range. The limited range of the standard train length or the unequal contribution of the two MMN generators mentioned above may contribute to the difference in the results. Further studies would be required to address this issue.

TMS has been used to study functional connectivity between two brain regions by dual-site stimulation or concurrent stimulation and brain imaging (Fox et al., 2012). In dual-site stimulation, the functional relationship between two regions is established by demonstrating that TMS on an association brain region influences the excitability of a primary motor or sensory region. The excitability of the primary motor or sensory region is typically measured by motor-evoked potential, motor threshold, or phosphene threshold triggered with a second TMS pulse. The functional connections of primary motor cortex with frontal or contralateral motor cortices (Civardi et al., 2001; Hanajima et al., 2001; van Campen et al., 2013), as well as connections of occipital visual regions with frontal eye field (Silvanto et al., 2006) or parietal cortex (Silvanto et al., 2009) have been studied with this approach. However, the frontal and temporal network underlying MMN cannot be studied with the dual stimulation method, due to the lack of a cortical excitability index for the auditory cortex.

Hence, a concurrent stimulation and brain imaging approach (e.g., Leitão et al., 2013; Mullin and Steeves, 2013; Parks et al., 2015; Ruff et al., 2006) was adopted in the current study. Top-down influence of posterior parietal cortex on visual cortex previously was shown by using concurrent TMS and EROS recording (Parks et al., 2015). Similar to the conclusion of these studies, a directional functional connection does not require a direct connection between IFC and STC in the current study. The functioning between the two brain regions could still be mediated through another brain region (i.e., an indirect connection of IFC to STC). However, with the temporal relationship between TMS and subsequent brain response taken into account, a directional functional connection of IFC followed-by, or leading to STC mismatch responses could be established.

Some ERP MMN studies revealed a lateralized MMN response, which seems to contradict the bilateral STC mismatch response assumption in the current study. However, these ERP studies investigated the change detection of emotion, (e.g., Schirmer and Escoffier, 2010), speech (e.g., Herrmann et al., 2009), or rhythm (e.g., Limb et al., 2006), which are known for lateralized brain responses. Additionally, the lateralized MMN responses observed in these studies does not necessarily imply lateralized STC mismatch responses, as the lateralized MMN responses may reflect combined bilateral STC and unilateral IFC mismatch responses. Bilateral STC mismatch responses to deviants with physical change were commonly found in fMRI (Leff et al., 2009; Szycik et al., 2013) and EROS (Tse and Penney, 2007); both methods provide superior spatial localization power to reveal hemispheric differences in IFC and STC mismatch responses.

In summary, the current study demonstrated a directional functional connectivity between IFC and STC in the change detection process of a passive oddball paradigm, which is a fundamental assumption underlying various hypotheses about the generation of MMN. Making use of the superior spatiotemporal localization abilities of both spTMS and EROS, and absence of electromagnetic inference between the two techniques, spTMS was applied on IFC to perturb its function while EROS was recorded from STC to observe the TMS effect on the subsequent mismatch response. It provides an example of the advantage of combining electromagnetic stimulation and optical brain imaging methods. Our results also provide support for a critical functional role of IFC in the pre-comparison stage of the change detection process and explain previous inconsistent findings in identifying the IFC generator of MMN.

Declaration of interest

S. F. W. Neggers is the owner of Brain Science Tools BV. The authors declare no conflict of interest otherwise.

Acknowledgements

Some aspects of this work were completed by L.-Y. Yip in partial fulfilment of the requirements for a Bachelor of Social Science degree at the Chinese University of Hong Kong. We wish to thank Cherry E. Frondozo, Kun-Yang Zhao, Qing-Hong Zeng, Geoffery C. S. Wong, Giovanna Tang, and Andy Lai for their technical support, and Lydia Yee and Trevor Penney for helpful comments on earlier versions of this manuscript. This project was supported by funding from the Early Career Scheme of the Research Grants Council (24401314) awarded to C.Y. Tse by the Hong Kong SAR University Grants Committee.

References

Alho, K., Woods, D.L., Algazi, A., 1994. Processing of auditory stimuli during auditory and visual attention as revealed by event-related potentials. Psychophysiology 31, 469–479.

Baldeweg, T., Klugman, A., Gruzelier, J., Hirsch, S.R., 2004. Mismatch negativity potentials and cognitive impairment in schizophrenia. Schizophr. Res. 69, 203–217. https://doi.org/10.1016/j.schres.2003.09.009.

Baudewig, J., Nitsche, M.A., Paulus, W., Frahm, J., 2001. Regional modulation of BOLD MRI responses to human sensorimotor activation by transcranial direct current stimulation. Magn. Reson. Med. 45, 196–201. https://doi.org/10.1002/1522-2594(200102)45:2<196::AID-MRM1026>3.0.CO;2–1.

Bendixen, A., Roeber, U., Schröger, E., 2007. Regularity extraction and application in dynamic auditory stimulus sequences. J. Cognit. Neurosci. 19, 1664–1677. https://doi.org/10.1162/jocn.2007.19.10.1664.

Bendixen, A., Schröger, E., 2008. Memory trace formation for abstract auditory features and its consequences in different attentional contexts. Biol. Psychol. 78, 231–241. https://doi.org/10.1016/j.biopsycho.2008.03.005.

Bestmann, S., Baudewig, J., Siebner, H.R., Rothwell, J.C., Frahm, J., 2004. Functional MRI of the immediate impact of transcranial magnetic stimulation on cortical and subcortical motor circuits. Eur. J. Neurosci. 19, 1950–1962. https://doi.org/10.1111/j.1460-9568.2004.03277.x.

Bohning, D.E., Shastri, A., Mcconnell, K. a, Nahas, Z., Lorberbaum, J.P., Roberts, D.R., Teneback, C., Vincent, D.J., George, M.S., 1999. A combined TMS/fMRI study of intensity-dependent TMS over motor cortex. Biol. Psychiatr. 45, 385–394.

Bonato, C., Miniussi, C., Rossini, P.M., 2006. Transcranial magnetic stimulation and cortical evoked potentials: a TMS/EEG co-registration study. Clin. Neurophysiol. 117, 1699–1707. https://doi.org/10.1016/j.clinph.2006.05.006.

Brainard, D.H., 1997. The psychophysics toolbox. Spatial Vis. 10, 433–436. https://doi.org/10.1163/156856897X00357.

Chen, J.C., Hämmerer, D., Strigaro, G., Liou, L.M., Tsai, C.H., Rothwell, J.C., Edwards, M.J., 2014. Domain-specific suppression of auditory mismatch negativity

with transcranial direct current stimulation. Clin. Neurophysiol. 125, 585–592. https://doi.org/10.1016/j.clinph.2013.08.007.
Civardi, C., Cantello, R., Asselman, P., Rothwell, J.C., 2001. Transcranial magnetic stimulation can be used to test connections to primary motor areas from frontal and medial cortex in humans. Neuroimage 14, 1444–1453. https://doi.org/10.1006/nimg.2001.0918.
Corthout, E., Uttl, B., Juan, C.H., Hallett, M., Cowey, A., 2000. Suppression of vision by transcranial magnetic stimulation: a third mechanism. Neuroreport 11, 2345–2349. https://doi.org/10.1097/00001756-200008030-00003.
Cox, R.W., 1996. AFNI: software for analysis and visualization of functional magnetic resonance neuroimages. Comput. Biomed. Res. 173, 162–173. http://doi.org/10.1006/cbmr.1996.0014.
Davey, N.J., Romaiguère, P., Maskill, D.W., Ellaway, P.H., 1994. Suppression of voluntary motor activity revealed using transcranial magnetic stimulation of the motor cortex in man. J. Physiol. 477, 223–235.
de Weijer, A.D., Sommer, I.E.C., Bakker, E.J., Bloemendaal, M., Bakker, C.J.G., Klomp, D.W.J., Bestmann, S., Neggers, S.F.W., 2014. A setup for administering TMS to medial and lateral cortical areas during whole-brain fMRI recording. J. Clin. Neurophysiol. 31, 474–487. https://doi.org/10.1097/WNP.0000000000000075.
Deouell, L.Y., 2007. The frontal generator of the mismatch negativity revisited. J. Psychophysiol. 21, 188–203. https://doi.org/10.1027/0269-8803.21.34.188.
Deouell, L.Y., Bentin, S., Giard, M.H., 1998. Mismatch negativity in dichotic listening: evidence for interhemispheric differences and multiple generators. Psychophysiology 35, 355–365. https://doi.org/10.1017/S0048577298970287.
Doeller, C.F., Opitz, B., Mecklinger, A., Krick, C., Reith, W., Schröger, E., 2003. Prefrontal cortex involvement in preattentive auditory deviance detection: neuroimaging and electrophysiological evidence. Neuroimage 20, 1270–1282. https://doi.org/10.1016/S1053-8119(03)00389-6.
Dürschmid, S., Edwards, E., Reichert, C., Dewar, C., Hinrichs, H., Heinze, H.-J., Kirsch, H.E., Dalal, S.S., Deouell, L.Y., Knight, R.T., 2016. Hierarchy of prediction errors for auditory events in human temporal and frontal cortex. Proc. Natl. Acad. Sci. Unit. States Am. 113, 6755–6760. https://doi.org/10.1073/pnas.1525030113.
Foust, A.J., Rector, D.M., 2007. Optically teasing apart neural swelling and depolarization. Neuroscience 145 (3), 887–899.
Fox, M.D., Halko, M.A., Eldaief, M.C., Pascual-Leone, A., 2012. Measuring and manipulating brain connectivity with resting state functional connectivity magnetic resonance imaging (fcMRI) and transcranial magnetic stimulation (TMS). Neuroimage 62, 2232–2243. https://doi.org/10.1016/j.neuroimage.2012.03.035.
Friston, K.J., 2010. The free-energy principle: a unified brain theory? Nat. Rev. Neurosci. 11, 127–138. https://doi.org/10.1038/nrn2787.
Friston, K.J., 2005. A theory of cortical responses. Philos. Trans. R. Soc. Lond. B Biol. Sci. 360, 815–836. https://doi.org/10.1098/rstb.2005.1622.
Friston, K.J., 2011. Functional and effective connectivity: a review. Brain Connect. 1, 13–36. https://doi.org/10.1089/brain.2011.0008.
Friston, K.J., Worsley, K.J., Frackowiak, R.S.J., Mazziotta, J.C., Evans, A.C., 1994. Assessing the significance of focal activations using their spatial extent. Hum. Brain Mapp. 1, 210–220. https://doi.org/10.1002/hbm.460010306.
Frühholz, S., Grandjean, D., 2013. Processing of emotional vocalizations in bilateral inferior frontal cortex. Neurosci. Biobehav. Rev. 37 (10), 2847–2855. http://doi.org/10.1016/j.neubiorev.2013.10.007.
Frühholz, S., Gschwind, M., Grandjean, D., 2015. Bilateral dorsal and ventral fiber pathways for the processing of affective prosody identified by probabilistic fiber tracking. Neuroimage 109, 27–34. http://doi.org/10.1016/j.neuroimage.2015.01.016.
Garrido, M.I., Friston, K.J., Kiebel, S.J., Stephan, K.E., Baldeweg, T., Kilner, J.M., 2008. The functional anatomy of the MMN: a DCM study of the roving paradigm. Neuroimage 42, 936–944. https://doi.org/10.1016/j.neuroimage.2008.05.018.
Garrido, M.I., Kilner, J.M., Kiebel, S.J., Friston, K.J., 2009. Dynamic causal modeling of the response to frequency deviants. J. Neurophysiol. 101, 2620–2631. https://doi.org/10.1152/jn.90291.2008.
Giard, M., Perrin, F., Pernier, J., Bouchet, P., 1990. Brain generators implicated in the processing of auditory stimulus deviance: a topographic event-related potential study. Psychophysiology 27, 627–640.
Graaf, T.A. De, Sack, A.T., 2011. Null results in TMS: from absence of evidence to evidence of absence. Neurosci. Biobehav. Rev. 35, 871–877. https://doi.org/10.1016/j.neubiorev.2010.10.006.
Gratton, G., 2018. Brain reflections: a circuit-based framework for understanding information processing and cognitive control. Psychophysiology 55. https://doi.org/10.1111/psyp.13038.
Gratton, G., 2010. Fast optical imaging of human brain function. Front. Hum. Neurosci. 4, 1–9. https://doi.org/10.3389/fnhum.2010.00052.
Gratton, G., 2000. Opt-cont" and "opt-3D": a software suite for the analysis and 3Dreconstruction of the event-related optical signal (EROS). Psychophysiology 37.
Gratton, G., Brumback, C.R., Gordon, B.A., Pearson, M.A., Low, K.A., Fabiani, M., 2006. Effects of measurement method, wavelength, and source-detector distance on the fast optical signal. Neuroimage 32, 1576–1590. https://doi.org/10.1016/j.neuroimage.2006.05.030.
Gratton, G., Fabiani, M., 2009. Fast optical signals: principles, methods, and experimental results. In: Frostig, R.D. (Ed.), In Vivo Optical Imaging of Brain. CRC Press, Boca Raton, FL, pp. 436–460.
Gratton, G., Fabiani, M., 2001. Shedding light on brain function: the event related optical signal. Trends Congnitive Sci. 5, 357–363. https://doi.org/10.1016/S1364-6613(00)01701-0.
Gratton, G., Corballis, P.M., 1995. Removing the heart from the brain: compensation for the pulse artifact in the photon migration signal. Psychophysiology 32, 292–299. https://doi.org/10.1111/j.1469-8986.1995.tb02958.x.
Gratton, G., Corballis, P.M., Euhee, C., Monica, F., Donald, C.H., 1995. Shades of gray matter: noninvasive optical images of human brain responses during visual stimulation. Psychophysiology 32, 505–509. https://doi.org/10.1111/j.1469-8986.1995.tb02102.x.
Hada, Y., Abo, M., Kaminaga, T., Mikami, M., 2006. Detection of cerebral blood flow changes during repetitive transcranial magnetic stimulation by recording hemoglobin in the brain cortex, just beneath the stimulation coil, with near-infrared spectroscopy. Neuroimage 32, 1226–1230. https://doi.org/10.1016/j.neuroimage.2006.04.200.
Haenschel, C., Vernon, D.J., Dwivedi, P., Gruzelier, J.H., Baldeweg, T., 2005. Event-related brain potential correlates of human auditory sensory memory-trace formation. J. Neurosci. 25, 10494–10501. https://doi.org/10.1523/JNEUROSCI.1227-05.2005.
Hanajima, R., Ugawa, Y., Machii, K., Mochizuki, H., Terao, Y., Enomoto, H., Furubayashi, T., Shiio, Y., Uesugi, H., Kanazawa, I., 2001. Interhemispheric facilitation of the hand motor area in humans. J. Physiol. 531, 849–859. https://doi.org/10.1111/j.1469-7793.2001.0849h.x.
Herrmann, B., Maess, B., Hasting, A.S., Friederici, A.D., 2009. Localization of the syntactic mismatch negativity in the temporal cortex: an MEG study. Neuroimage 48, 590–600. https://doi.org/10.1016/j.neuroimage.2009.06.082.
Hofer, S., Frahm, J., 2006. Topography of the human corpus callosum revisited-Comprehensive fiber tractography using diffusion tensor magnetic resonance imaging. Neuroimage 32 (3), 989–994. http://doi.org/10.1016/j.neuroimage.2006.05.044.
Horváth, J., Czigler, I., Jacobsen, T., Maess, B., Schröger, E., Winkler, I., 2008. MMN or no MMN: no magnitude of deviance effect on the MMN amplitude. Psychophysiology 45, 60–69. https://doi.org/10.1111/j.1469-8986.2007.00599.x.
Ilmoniemi, R.J., Virtanen, J., Ruohonen, J., Karhu, J., Aronen, H.J., Näätänen, R., Katila, T., 1997. Neuronal responses to magnetic stimulation reveal cortical reactivity and connectivity. Neuroreport 8, 3537–3540. https://doi.org/10.1097/00001756-199711100-00024.
Impey, D., Knott, V., 2015. Effect of transcranial direct current stimulation (tDCS) on MMN- indexed auditory discrimination: a pilot study. J. Neural. Transm. 1175–1185. https://doi.org/10.1007/s00702-015-1365-9.
Jacobsen, T., Schröger, E., 2001. Is there pre-attentive memory-based comparison of pitch? Psychophysiology 38, 723–727.
Kozel, F.A., Tian, F., Dhamne, S., Croarkin, P.E., McClintock, S.M., Elliott, A., Kimberly, S.M., Mustafa, H., Liu, H., 2009. Using simultaneous repetitive transcranial magnetic stimulation/functional near infrared spectroscopy (rTMS/fNIRS) to measure brain activation and connectivity. Neuroimage 47, 1177–1184. https://doi.org/10.1016/j.neuroimage.2009.05.016.
Lappe, C., Steinsträter, O., Pantev, C., 2013a. Rhythmic and melodic deviations in musical sequences recruit different cortical areas for mismatch detection. Front. Hum. Neurosci. 7, 1–9. https://doi.org/10.3389/fnhum.2013.00260.
Lappe, C., Steinsträter, O., Pantev, C., 2013b. A beamformer analysis of MEG data reveals frontal generators of the musically elicited mismatch negativity. PLoS One 8, 25–31. https://doi.org/10.1371/journal.pone.0061296.
Leff, A.P., Iverson, P., Schofield, T.M., Kilner, J.M., Crinion, J.T., Friston, K.J., Price, C.J., 2009. Vowel-specific mismatch responses in the anterior superior temporal gyrus: an fMRI study. Cortex 45, 517–526. https://doi.org/10.1016/j.cortex.2007.10.008.
Leitão, J., Thielscher, A., Werner, S., Pohmann, R., Noppeney, U., 2013. Effects of parietal TMS on visual and auditory processing at the primary cortical level-a concurrent TMS-fMRI study. Cerebr. Cortex 23, 873–884. https://doi.org/10.1093/cercor/bhs078.
Liebenthal, E., Ellingson, M.L., Spanaki, M.V., Prieto, T.E., Ropella, K.M., Binder, J.R., 2003. Simultaneous ERP and fMRI of the auditory cortex in a passive oddball paradigm. Neuroimage 19, 1395–1404. https://doi.org/10.1016/S1053-8119(03)00228-3.
Limb, C.J., Kemeny, S., Ortigoza, E.B., Rouhani, S., Braun, A.R., 2006. Left hemispheric lateralization of brain activity during passive rhythm perception in musicians. Anat. Rec. Part A Discov. Mol. Cell. Evol. Biol. 288, 382–389. https://doi.org/10.1002/ar.a.20298.
MacLean, S.E., Blundon, E.G., Ward, L.M., 2015. Brain regional networks active during the mismatch negativity vary with paradigm. Neuropsychologia 75, 242–251. https://doi.org/10.1016/j.neuropsychologia.2015.06.019.
Mochizuki, H., Ugawa, Y., Terao, Y., Sakai, K.L., 2006. Cortical hemoglobin-concentration changes under the coil induced by single-pulse TMS in humans: a simultaneous recording with near-infrared spectroscopy. Exp. Brain Res. 169, 302–310. https://doi.org/10.1007/s00221-005-0149-0.
Molholm, S., Martinez, A., Ritter, W., Javitt, D.C., Foxe, J.J., 2005. The neural circuitry of pre-attentive auditory change-detection: an fMRI study of pitch and duration mismatch negativity generators. Cerebr. Cortex 15, 545–551. https://doi.org/10.1093/cercor/bhh155.
Möttönen, R., Dutton, R., Watkins, K.E., 2013. Auditory-motor processing of speech sounds. Cerebr. Cortex 23, 1190–1197. https://doi.org/10.1093/cercor/bhs110.
Mullin, C.R., Steeves, J.K.E., 2013. Consecutive TMS-fMRI reveals an inverse relationship in BOLD signal between object and scene processing. J. Neurosci. 33, 19243–19249. https://doi.org/10.1523/JNEUROSCI.2537-13.2013.
Näätänen, R., Michie, P.T., 1979. Early selective-attention effects on the evoked potential: a critical review and reinterpretation. Biol. Psychol. 8, 81–136.
Näätänen, R., Paavilainen, P., Rinne, T., Alho, K., 2007. The mismatch negativity (MMN) in basic research of central auditory processing: a review. Clin. Neurophysiol. 118, 2544–2590. https://doi.org/10.1016/j.clinph.2007.04.026.
Neggers, S.F.W., Langerak, T.R., Schutter, D.J.L.G., Mandl, R.C.W., Ramsey, N.F., Lemmens, P.J.J., Postma, A., 2004. A stereotactic method for image-guided transcranial magnetic stimulation validated with fMRI and motor-evoked potentials. Neuroimage 21, 1805–1817. https://doi.org/10.1016/j.neuroimage.2003.12.006.

Oldfield, R.C., 1971. The assessment and analysis of handedness: the edinburgh inventory. Neuropsychologia 9, 97–113. https://doi.org/10.1016/0028-3932(71)90067-4.

Opitz, B., Rinne, T., Mecklinger, A., Von Cramon, D.Y., Schröger, E., 2002. Differential contribution of frontal and temporal cortices to auditory change detection: FMRI and ERP results. Neuroimage 15, 167–174. https://doi.org/10.1006/nimg.2001.0970.

Oshima, H., Shiga, T., Niwa, S., Enomoto, H., Ugawa, Y., Yabe, H., 2017. Alteration of duration mismatch negativity induced by transcranial magnetic stimulation over the left parietal lobe. Clin. EEG Neurosci. 48, 11–19. https://doi.org/10.1177/1550059416630483.

Parks, N.A., 2013. Concurrent application of TMS and near-infrared optical imaging: methodological considerations and potential artifacts. Front. Hum. Neurosci. 7, 1–10. https://doi.org/10.3389/fnhum.2013.00592.

Parks, N.A., Maclin, E.L., Low, K.A., Beck, D.M., Fabiani, M., Gratton, G., 2012. Examining cortical dynamics and connectivity with simultaneous single-pulse transcranial magnetic stimulation and fast optical imaging. Neuroimage 59, 2504–2510. https://doi.org/10.1109/TMI.2012.2196707.Separate.

Parks, N.A., Mazzi, C., Tapia, E., Savazzi, S., Fabiani, M., Gratton, G., Beck, D.M., 2015. The influence of posterior parietal cortex on extrastriate visual activity: a concurrent TMS and fast optical imaging study. Neuropsychologia 78, 153–158.

Phillips, H.N., Blenkmann, A., Hughes, L.E., Kochen, S., Bekinschtein, T.A., Cam, C.A.N., Rowe, J.B., 2016. Convergent evidence for hierarchical prediction networks from human electrocorticography and magnetoencephalography. Cortex 82, 192–205. https://doi.org/10.1016/j.cortex.2016.05.001.

Plewnia, C., Bartels, M., Gerloff, C., 2003. Transient suppression of tinnitus by transcranial magnetic stimulation. Ann. Neurol. 53, 263–266.

Rector, D.M., Carter, K.M., Volegov, P.L., George, J.S., 2005. Spatio-temporal mapping of rat whisker barrels with fast scattered light signals. Neuroimage 26 (2), 619–627.

Rector, D.M., Poe, G.R., Kristensen, M.P., Harper, R.M., 1997. Light scattering changes follow evoked potentials from hippocampal schaeffer collateral stimulation. J. Neurophysiol. 78 (3), 1707–1713.

Rinne, T., Alho, K., Ilmoniemi, R.J., Virtanen, J., Näätänen, R., 2000. Separate time behaviors of the temporal and frontal mismatch negativity sources. Neuroimage 12, 14–19. https://doi.org/10.1006/nimg.2000.0591.

Rinne, T., Degerman, A., Alho, K., 2005. Superior temporal and inferior frontal cortices are activated by infrequent sound duration decrements: an fMRI study. Neuroimage 26, 66–72. https://doi.org/10.1016/j.neuroimage.2005.01.017.

Rinne, T., Gratton, G., Fabiani, M., Cowan, N., Maclin, E., Stinard, A., Sinkkonen, J., Alho, K., Näätänen, R., 1999. Scalp-recorded optical signals make sound processing in the auditory cortex visible? Neuroimage 10, 620–624. https://doi.org/10.1006/nimg.1999.0495.

Rossi, S., Hallett, M., Rossini, P.M., Pascual-leone, A., 2009. Safety, ethical considerations, and application guidelines for the use of transcranial magnetic stimulation in clinical practice and research. Clin. Neurophysiol. 120, 2008–2039. https://doi.org/10.1016/j.clinph.2009.08.016.

Ruff, C.C., Blankenburg, F., Bjoertomt, O., Bestmann, S., Freeman, E., Haynes, J.D., Rees, G., Josephs, O., Deichmann, R., Driver, J., 2006. Concurrent TMS-fMRI and psychophysics reveal frontal influences on human retinotopic visual cortex. Curr. Biol. 16, 1479–1488. https://doi.org/10.1016/j.cub.2006.06.057.

Sable, J.J., Low, K.A., Whalen, C.J., Maclin, E.L., Fabiani, M., Gratton, G., 2007. Optical imaging of temporal integration in human auditory cortex. Eur. J. Neurosci. 25, 298–306. https://doi.org/10.1111/j.1460-9568.2006.05255.x.

Scherg, M., Vajsar, J., Picton, T.W., 1989. A source analysis of the late human auditory evoked potentials. J. Cognit. Neurosci. 1, 336–355. https://doi.org/10.1162/jocn.1989.1.4.336.

Schirmer, A., Escoffier, N., 2010. Emotional MMN: anxiety and heart rate correlate with the ERP signature for auditory change detection. Clin. Neurophysiol. 121, 53–59. https://doi.org/10.1016/j.clinph.2009.09.029.

Shalgi, S., Deouell, L.Y., 2007. Direct evidence for differential roles of temporal and frontal components of auditory change detection. Neuropsychologia 45, 1878–1888. https://doi.org/10.1016/j.neuropsychologia.2006.11.023.

Silvanto, J., Lavie, N., Walsh, V., 2006. Stimulation of human frontal eye fields modulates sensitivity of extrastriate visual cortex. J. Neurophysiol. 15–2006 https://doi.org/10.1152/jn.00015.2006.The.

Silvanto, J., Muggleton, N., Lavie, N., Walsh, V., 2009. The perceptual and functional consequences of parietal top-down modulation on the visual cortex. Cerebr. Cortex 19, 327–330. https://doi.org/10.1093/cercor/bhn091.

Szycik, G.R., Stadler, J., Brechmann, A., Münte, T.F., 2013. Preattentive mechanisms of change detection in early auditory cortex: a 7 Tesla fMRI study. Neuroscience 253, 100–109. https://doi.org/10.1016/j.neuroscience.2013.08.039.

Talairach, J., Tournoux, P., 1988. A Co-planar Stereotaxic Atlas of a Human Brain.

Tiitinen, H., May, P., Reinikainen, K., Näätänen, R., 1994. Attentive novelty detection in humans is governed by pre-attentive sensory memory. Nature 372, 90–92. https://doi.org/10.1038/372090a0.

Tse, C.-Y., Gratton, G., Garnsey, S.M., Novak, M.A., Fabiani, M., 2015. Read my lips: brain dynamics associated with audiovisual integration and deviance detection. J. Cognit. Neurosci. 27, 1723–1737. https://doi.org/10.1162/jocn_a_00812.

Tse, C.-Y., Low, K.A., Fabiani, M., Gratton, G., 2012. Rules rule! brain activity dissociates the representations of stimulus contingencies with varying levels of complexity. J. Cognit. Neurosci. 24, 1941–1959. https://doi.org/10.1162/jocn.

Tse, C.-Y., Penney, T.B., 2008. On the functional role of temporal and frontal cortex activation in passive detection of auditory deviance. Neuroimage 41, 1462–1470. https://doi.org/10.1016/j.neuroimage.2008.03.043.

Tse, C.-Y., Penney, T.B., 2007. Preattentive change detection using the event-related optical signal. IEEE Eng. Med. Biol. Mag. 26, 52–58. https://doi.org/10.1109/MEMB.2007.384096.

Tse, C.-Y., Tien, K.-R., Penney, T.B., 2006. Event-related optical imaging reveals the temporal dynamics of right temporal and frontal cortex activation in pre-attentive change detection. Neuroimage 29, 314–320. https://doi.org/10.1016/j.neuroimage.2005.07.013.

Tse, C.-Y., Gordon, B.A., Fabiani, M., Gratton, G., 2010. Frequency analysis of the visual steady-state response measured with the fast optical signal in younger and older adults. Biol. Psychol. 85, 79–89. https://doi.org/10.1016/j.biopsycho.2010.05.007.Frequency.

Tse, C.-Y., Rinne, T., Ng, K.K., Penney, T.B., 2013. The functional role of the frontal cortex in pre-attentive auditory change detection. Neuroimage 83, 870–879. https://doi.org/10.1016/j.neuroimage.2013.07.037.

van Campen, A.D., Neubert, F.-X., van den Wildenberg, W.P.M., Ridderinkhof, K.R., Mars, R.B., 2013. Paired-pulse transcranial magnetic stimulation reveals probability-dependent changes in functional connectivity between right inferior frontal cortex and primary motor cortex during go/no-go performance. Front. Hum. Neurosci. 7 (736). https://doi.org/10.3389/fnhum.2013.00736.

Van Ettinger-Veenstra, H.M., Huijbers, W., Gutteling, T.P., Vink, M., Kenemans, J.L., Neggers, S.F.W., 2009. fMRI-Guided TMS on cortical eye fields: the frontal but not intraparietal eye fields regulate the coupling between visuospatial attention and eye movements. J. Neurophysiol. 102, 3469–3480. https://doi.org/10.1152/jn.00350.2009.

Vossel, S., Weidner, R., Fink, G.R., 2011. Dynamic coding of events within the inferior frontal gyrus in a probabilistic selective attention task. J. Cognit. Neurosci. 23, 414–424. https://doi.org/10.1162/jocn.2010.21441.

Wassermann, E.M., 1998. Risk and safety of repetitive transcranial magnetic stimulation : report and suggested guidelines from the international workshop on the safety of repetitive transcranial magnetic stimulation, june 5 – 7, 1996. Electroencephalogr. Clin. Neurophysiol. 108, 1–16.

Weigl, M., Mecklinger, A., Rosburg, T., 2016. Transcranial direct current stimulation over the left dorsolateral prefrontal cortex modulates auditory mismatch negativity. Clin. Neurophysiol. 127, 2263–2272. https://doi.org/10.1016/j.clinph.2016.01.024.

Whalen, C., Maclin, E.L., Fabiani, M., Gratton, G., 2008. Validation of a method for coregistering scalp recording locations with 3D structural MR images. Hum. Brain Mapp. 29, 1288–1301. https://doi.org/10.1002/hbm.20465.

Winkler, I., 2007. Interpreting the mismatch negativity. J. Psychophysiol. 21, 147–163. https://doi.org/10.1027/0269-8803.21.3.147.

Winkler, I., Cowan, N., Czigler, V.C., I., Näätänen, R., 1996. Interaction between transient and long-term auditory memory as reflected by the mismatch negativity. J. Cognit. Neurosci. 8, 403–415.

Wolf, U., Wolf, M., Toronov, V., Michalos, A., Paunescu, L.A., Gratton, E., 2000. Detecting cerebral functional slow and fast signals by frequency-domain near-infrared spectroscopy using two different sensors. Biomed. Opt. Spectrosc. Diagn. 1–4.